Using bidirectional modulation of 2-Ch phase modulator as basis for nonlinear distortion compensation in analog photonic links

Jian Niu (牛 剑), Kun Xu (徐 坤)*, Xiaojun Xie (谢小军), Yitang Dai (戴一堂), Jianqiang Li (李建强), Yuefeng Ji (纪越峰), and Jintong Lin (林金桐)

State Key Laboratory of Information Photonics and Optical Communications, Beijing University of Posts and Telecommunications, Beijing 100876, China

**Corresponding author: xukun@bupt.edu.cn*

Received March 13, 2013; accepted May 13, 2013; posted online July 26, 2013

We propose a third-order intermodulation distortion (IMD3) compensation scheme based on the bidirectional modulation of 2-Ch phase modulator (PM). We realize the destructive combination of IMD3 by using different modulation efficiencies and appropriately adjusting the input optical power ratio to satisfy a fixed relationship with modulation efficiency. The primary advantage of this scheme is that out-of-phase IMD3 is introduced using only one 2-Ch PM, thereby resulting in the cancellation of IMD3. Up to 27-dB suppression in IMD3 is experimentally demonstrated—a feature that will be useful in low-distortion analog optical transmission.

OCIS codes: 060.0060, 060.2330.

doi: 10.3788/COL201311.080603.

Analog photonic links (APLs) are actively developed as substitutes for conventional electromagnetic transmission lines in numerous applications, such as phased-array antennas, signal processing, radar systems, radio-over-fiber, and radio astronomy[1,2]. Given that third-order intermodulation distortion (IMD3) dominates link distortions and constrains the spurious-free dynamic range (SFDR), several techniques have been developed to suppress IMD3 and improve the SFDR of APLs; these techniques include broadband radio frequency (RF) predistortion circuit[3], optical feed-forward system[4], post-compensation method[5], and digital post-processing[6]. In Ref. [3], a predistortion circuit is accurately designed and fabricated to offset the nonlinearity of the transfer function of electroabsorption modulator (EAMs). The basic structure of feed-forward linearization in Ref. [4] is characterized by two cancellation loops: the carrier signal and error cancellation loops. For broadband and significant suppression, the amplitude and phase match, as well as the equality of signal delays among different branches, should be accurately controlled. A reflective optical arbitrary waveform generator is required to implement the spectral line-by-line processing of intensity-modulated signals; such processing causes two types of IMD3 origins to have equal intensity and cancel each other out[5]. Multiscale sampling combined with digital post-processing has been used to extend the dynamic range of optically filtered analog photonic systems[6]. Based on digital post-processing, the phase-modulation I/Q-demodulation method presented by Clark *et al*. has attracted increasing attention over the past few years[7,8] Complex digital signal processing and limited processing speed restrict system bandwidth. The methods based on the use of the Mach–Zehnders[9] and parallel Mach–Zehnders[10] series were proposed to realize link linearization and low-distortion analog optical transmission. The idea is to arrange the distortion produced by a second modulator to be equal in magnitude but out of phase with the distortion produced by the first modulator, thereby canceling the distortion from the combined device. Despite the benefits of this approach, using two modulators increases cost and complexity. Similar to the linearization principle that uses parallel Mach–Zehnders, the dual parallel Mach–Zehnder modulator (DPMZM) has been used to generate broadband-linearized optical single-sideband signals and highly linear vector modulation signal transmission in radio-over-fiber systems[11].

In this letter, we use a destructive combination principle that uses only one-phase modulator (PM) as basis in developing an IMD3 compensation scheme. In theory, the modulation efficiencies of a 2-Ch PM differ at opposite directions. If the input optical power ratio is adjusted to satisfy a fixed relationship with modulation efficiency, then IMD3 is destructively combined and completely suppressed. An out-of-phase IMD3 is introduced by using only one 2-Ch PM, resulting in the cancellation of IMD3. We demonstrate up to 27-dB IMD3 suppression, with linear terms experiencing only little attenuation.

Figure 1 shows the schematic of the IMD3 compensation method based on the bidirectional modulation of 2-Ch PMs. With a tunable optical coupler (TOC), the optical carrier is split into two branches and then sent to the first input port of circulators with appropriate polarization orientations of θ_1 and θ_2 to the y-axis; the orientations are derived by adjusting the polarization controllers (PC1 and PC2). At ports 2 and 2', the optical carriers are reversely launched into the 2-Ch PM driven by the RF signal. The 2-Ch PM developed by Versawave Technologies supports both the TE and TM modes with contrasting PM indexes, similar to that implemented in the polarization modulator discussed in Ref. [12]. Given that the 2-Ch PM has different responsivities for the optical waves that co-propagate (forward) and counter-propagate (reverse) to the RF signal, modulation half-wave voltages differ and are characterized by the following relationship[13]:

$$V_{\pi,\mathrm{rev}} = V_{\pi,\mathrm{for}}\left[\Omega\tau/\sin(\Omega\tau)\right]=V_{\pi,\mathrm{for}}\kappa, \quad (1)$$

where $V_{\pi,\mathrm{for}}$ and $V_{\pi,\mathrm{rev}}$ are the half-wave voltages for the forward- and reverse-traveling optical waves, respectively; Ω is the angular frequency of the input RF signal; τ is the signal transit time in the traveling-wave modulator. Thus, the modulated signals can be expressed as

$$\begin{aligned}\left[\begin{array}{c} E_1(t) \\ E_2(t) \end{array}\right] &= \left[\begin{array}{c} \sqrt{P_1}\mathrm{e}^{\mathrm{j}\omega t}(\widehat{y}\cos\theta_1 \mathrm{e}^{\mathrm{j}\pi V_0\cos(\Omega t)/V_{\pi,\,\mathrm{for}}}+\widehat{x}\sin\theta_1\mathrm{e}^{-\mathrm{j}\pi V_0\cos(\Omega t)/V_{\pi,\,\mathrm{for}}}) \\ \sqrt{P_2}\mathrm{e}^{\mathrm{j}\omega t}(\widehat{y}\cos\theta_2 \mathrm{e}^{\mathrm{j}\pi V_0\cos(\Omega t)/V_{\pi,\,\mathrm{rev}}}+\widehat{x}\sin\theta_2\mathrm{e}^{-\mathrm{j}\pi V_0\cos(\Omega t)/V_{\pi,\,\mathrm{rev}}}) \end{array}\right] \\ &= \left[\begin{array}{c} \sqrt{P_1}\mathrm{e}^{\mathrm{j}\omega t}(\widehat{y}\cos\theta_1 \mathrm{e}^{\mathrm{j}\beta\cos(\Omega t)}+\widehat{x}\sin\theta_1\mathrm{e}^{-\mathrm{j}\beta\cos(\Omega t)}) \\ \sqrt{P_2}\mathrm{e}^{\mathrm{j}\omega t}(\widehat{y}\cos\theta_2 \mathrm{e}^{\mathrm{j}\beta\cos(\Omega t)/\kappa}+\widehat{x}\sin\theta_2\mathrm{e}^{-\mathrm{j}\beta\cos(\Omega t)/\kappa}) \end{array}\right]. \end{aligned} \quad (2)$$

The modulated optical signals are routed to the third port of circulators and sent to the polarization selective element that comprises a PC and polarizer. The two polarizers aligned at α_1 and α_2 relative to the y-axis and the polarization axis are denoted as $\widehat{J}_1$ and $\widehat{J}_2$, respectively. The output optical fields are derived thus:

$$\left[\begin{array}{c} E_1(t) \\ E_2(t) \end{array}\right] = \left[\begin{array}{c} \sqrt{P_1}\mathrm{e}^{\mathrm{j}\omega t}(\cos\theta_1\cos\alpha_1\mathrm{e}^{\mathrm{j}\beta\cos(\Omega t)}+\sin\theta_1\sin\alpha_1\mathrm{e}^{-\mathrm{j}\beta\cos(\Omega t)})\widehat{J}_1 \\ \sqrt{P_2}\mathrm{e}^{\mathrm{j}\omega t}(\cos\theta_2\cos\alpha_2\mathrm{e}^{\mathrm{j}\beta\cos(\Omega t)/\kappa}+\sin\theta_2\sin\alpha_2\mathrm{e}^{-\mathrm{j}\beta\cos(\Omega t)/\kappa})\widehat{J}_2 \end{array}\right]. \quad (3)$$

If α_2=$\alpha_1 \pm \pi/2$, condition $\widehat{J}_1 \perp \widehat{J}_2$ holds. Thus, the two optical fields are incoherent, and the output optical power is

$$\left[\begin{array}{c} P_{1\mathrm{out}} \\ P_{2\mathrm{out}} \end{array}\right] = \left[\begin{array}{c} P_1\left\{\cos^2\theta_1\cos^2\alpha_1+\sin^2\theta_1\sin^2\alpha_1+\sin 2\theta_1\sin 2\alpha_1\cos\left[2\beta cos(\Omega t)/2\right]\right\} \\ P_2\left\{\cos^2\theta_2\cos^2\alpha_2+\sin^2\theta_2\sin^2\alpha_2+\sin 2\theta_2\sin 2\alpha_2\cos\left[2\beta cos(\Omega t)/\kappa\right]/2\right\} \end{array}\right]. \quad (4)$$

The equivalent incoherent combination of the two optical signals is achieved after 3-dB coupling. Following photoelectric conversion, considering θ_1=θ_2=α_1=$\pi/4$ and α_2 =$-\pi/4$, the RF photocurrent at the output port of the detector is destructively combined and can be given by

$$\begin{aligned} I &\propto P_1\sin\left[2\beta\cos(\Omega t)\right]-P_2\sin\left[2\beta\cos(\Omega t)/\kappa\right] \\ &= P_1 2\beta\cos(\Omega t)-\frac{P_2 2\beta}{\kappa}\cos(\Omega t) \\ &-\frac{1}{6}\left[2\beta\cos(\Omega t)\right]^3-\frac{1}{6}\left[\frac{2\beta}{\kappa}\cos(\Omega t)\right]^3+\cdots . \end{aligned} \quad (5)$$

When the input signal is set as a two-tone RF signal, disregarding higher order terms yields

$$\begin{aligned} I &\propto P_1\sin\left\{2\beta\left[\cos(\Omega_1 t)+\cos(\Omega_2 t)\right]\right\} \\ &-P_2\sin\left\{2\beta\left[\cos(\Omega_1 t)+\cos(\Omega_2 t)\right]/\kappa\right\} \\ &= (2P_1\beta-\frac{2P_2\beta}{\kappa}-3P_1\beta^3+3\frac{P_2\beta^3}{\kappa^3}) \\ &\cdot\left[\cos(\Omega_1 t)+\cos(\Omega_2 t)\right]-\frac{1}{3}(P_1\beta^3-\frac{P_2\beta^3}{\kappa^3}) \\ &\cdot\left[\cos(3\Omega_1 t)+\cos(3\Omega_2 t)\right]-(P_1\beta^3-\frac{P_2\beta^3}{\kappa^3}) \\ &\cdot\left[\cos(2\Omega_1+\Omega_2)t+\cos(2\Omega_2+\Omega_1)t\right. \\ &\left.+\cos(2\Omega_1-\Omega_2)t+\cos(2\Omega_2-\Omega_1)t\right]. \end{aligned} \quad (6)$$

According to Eq. (6), if the coefficient of the nonlinear terms equals 0 as the attenuation of linear terms are kept low, the following relationship should be satisfied:

$$P_2/P_1 = k^3, \quad k \neq 1. \quad (7)$$

Given that k is generally not equal to 1 in our scheme, adjusting the optical power ratio implemented by the TOC to satisfy $P_2/P_1 = k^3$ completely eliminates the IMD3 that usually limits the dynamic range.

To demonstrate the proposed scheme, we conduct a proof-of-concept experiment using the configurations shown in Fig. 1. The light from the laser source (NKT Photonics) is first separated and then adjusted by the TOC (FIBERPRO TDC1443451028). Given that the alignment accuracy of the TOC is limited, additional polarizers and PCs are inserted after PC1 and PC2 to

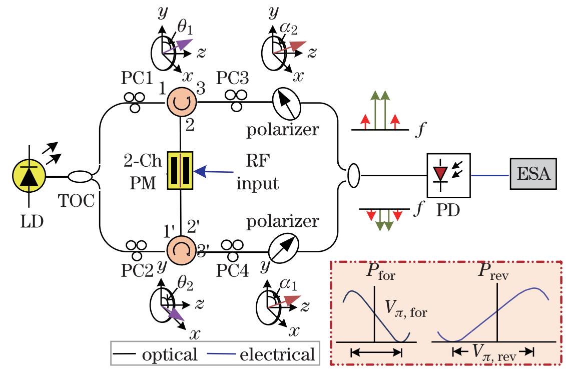

Fig. 1. Schematic of the proposed IMD3 compensation scheme. LD: laser diode; PD: photodetector; ESA: electrical signal analyzer. The inset depicts output power as a function of the applied voltage for the 2-Ch PM in opposite directions.

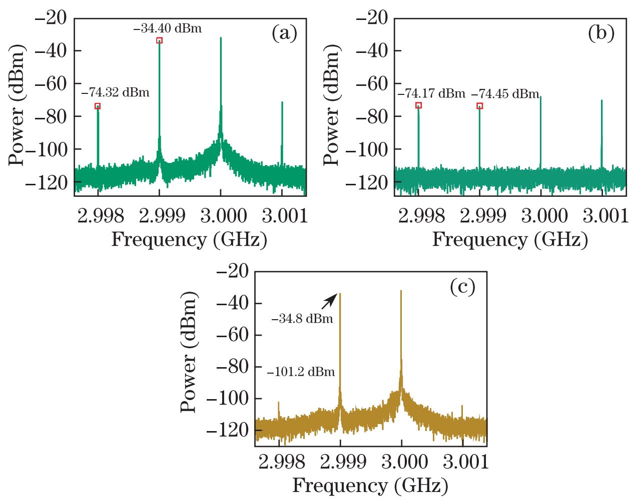

Fig. 2. Spectrum analyzer traces for the two-tone IMD3 test. (a) Counter-propagating trace; (b) co-propagating trace; (c) after the compensation of nonlinearity.

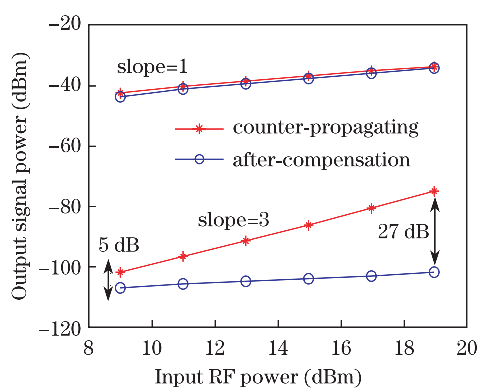

Fig. 3. Output signal power versus input RF power for counter-propagating and dispersion compensation links.

further align the two optical power levels injected into two ports of the 2-Ch PM. The 2-Ch PM is driven by two equal-amplitude RF tones with frequencies of 2.999 and 3 GHz. Two low-noise amplifiers are inserted before the RF signal is sent to the 2-Ch PM. After bidirectional modulation and polarization selection, the modulated signals are coupled and sent to the detector to realize optical-to-electrical conversion and destructive combination. The output signal is observed using an electrical signal analyzer (Anritsu MS2690A).

We can obtain output spectrum characteristics (Fig. 2) before and after IMD3 compensation. Figure 2(a) shows the counter-propagating trace. IMD3 is severe because of the nonlinear modulation characteristics. The same phenomenon is observed for the co-propagation trace (Fig. 2(b)). The IMD3 amplitudes of the two traces are almost identical to each other; i.e., about −74 dBm. By contrast, the amplitudes of the fundamental signals considerably differ from each other; i.e., −34.4 and −74.45 dBm. After destructive combination in the detector, 26.88-dB IMD3 suppression is achieved. Only about 0.4 dB sacrifice for the fundamental signal compared with that applied before IMD3 compensation (Fig. 2(c)).

We also analyze the relationship among the input RF signal power, output fundamental RF signal power, and output IMD3 power before and after the nonlinear distortion compensation with the two-tone RF signal. In Fig. 3, the two upper lines with slope = 1 represent the fundamental signal tone, and the two lower lines represent the IMD3 power. Without IMD3 compensation, the IMD3 power increases with the slope of three versus the power of the input RF signal. Nevertheless, after IMD3 compensation, the IMD3 power remains almost unchanged because the IMD3 is constantly suppressed. As shown in Fig. 3, the IMD3 is effectively suppressed up to 27 dB. Meanwhile, the power of the fundamental signal before and after distortion compensation remains almost constant, but because of destructive combination, small attenuation occurs after distortion compensation; this result is consistent with the principle analysis in part 2 and the analysis of Fig. 2. As indicated by the experimental results and analysis, IMD3 suppression up to 27 dB indicates the feasibility of applying the IMD3 compensation scheme in APLs.

In conclusion, we experimentally demonstrate an IMD3 compensation scheme based on the bidirectional modulation of 2-CH PM. By using the destructive combination of IMD3 in bidirectional modulation, we achieve a reduction of 27 dB in IMD3.

This work was supported by the National “863” Program of China (No. 2011AA010306), the National “973” Program of China (No. 2012CB315705), the National Natural Science Foundation of China (Nos. 61271042, 61107058, and 61120106001), the Beijing Excellent Doctoral Thesis Project (No. YB20101001301), the BUPT Excellent Ph.D. Students Foundation (No. CX201221), the Cooperation Project between Province and Ministries (No. 2011A090200025), and the Fundamental Research Funds for the Central Universities.

References

1. C. H. Cox, *Analog Optical Links: Theory and Practice* (Cambridge University Press, Cambridge, 2004).
2. V. J. Urick, in *Proceedings of OFC/NFOEC 2010* OML5 (2010).
3. Y. Shen, B. Hraimel, X. Zhang, G. E. R. Cowan, K. Wu, and T. Liu, IEEE Trans. Microw. Theory Technol. **58,** 3327 (2010).
4. Y.-T. Moon, J. W. Jang, W.-K. Choi, and Y.-W. Choi,

Opt. Express **15,** 12167 (2007).

5. G. Zhang, X. Zheng, S. Li, H. Zhang, and B. Zhou, Opt. Lett. **37,** 806 (2012).
6. A. Agarwal, T. Banwell, J. Jackel, P. Toliver, and T. K. Woodward, in *Proceedings of OFC 2009* OMI3 (2009).
7. T. R. Clark Jr and M. L. Dennis, in *Proceedings of MWP/APMP2008* 12 (2008).
8. T. R. Clark, S. R. O'Connor, and M. L. Dennis, IEEE Trans. Microw. Theory Technol. **58,** 3039 (2010).
9. H. Skeie and R. V. Johnsonnol, Proc. SPIE **1583,** 153 (1991).
10. S. K. Korotky and R. M. de Ridder, IEEE J. Sel. Area Commun. **8,** 1377 (1990).
11. J. Yu, S. Li, X. Zheng, H. Zhang, and B. Zhou, Chin. Opt. Lett. **10,** 100606 (2012).
12. J. D. Bull, J. D. Bull, N. A. F. Jaeger, H. Kato, M. Fairburn, A. Reid, and P. Ghanipour, Proc. SPIE **5557,** 133 (2004).
13. M. Y. Frankel and R. D. Esman, J. Lightwave Technol. **16,** 859 (1998).